Attenuating multiples with the restricted domain hyperbolic Radon transform

Juan I. Sabbione (University of Alberta)* and Mauricio D. Sacchi (University of Alberta).

Abstract

We present a study that illustrates how to attenuate multiples using the restricted domain hyperbolic Radon transform (RHRT). The classical hyperbolic Radon transform (HRT) entails solving an inverse problem with a large number Radon coefficients. As opposed to HRT, in RHRT a small subset of the velocity panel is used to model the data. This subset is defined adaptively for each common-midpoint gather (CMP) using a velocity panel bitmap, which is determined by the amplitudes of the adjoint Radon coefficients. This strategy helps to speed up computation of the transform and to enhance the focusing on the model domain. A well-studied marine data set from the Gulf of Mexico is processed to assess the performance of the method. The data is severely contaminated with multiple reflections and peglegs due to a shallow salt body intrusion. The proposed method successfully removes most of the multiples energy revealing greater details in the final section and improving the continuity of the deep reflectors and diffractions.

Introduction

In marine seismic exploration, multiple suppression represents an essential step in several processing sequences. There are plenty of alternative methods to address the problem. Among them, the most widely used can be divided into those that build a model that predicts the multiples and then remove them from the data (Verschuur et al., 1992; Berkhout and Verschuur, 1997), and those that separate multiples from primaries in the Radon domain, often adopting a high-resolution transform (Sacchi and Ulrych, 1995).

The Radon transform emerged a few decades ago as a processing method for velocity analysis (Thorson, 1985) and multiple suppression (Hampson, 1986; Foster, 1992). Currently, Radon transforms remain popular techniques to tackle a collection of processing tasks in seismic exploration due to their simplicity and flexibility. Moreover, new applications involving different settings of the Radon transform have been proposed in very recent years. They include separation of simultaneous sources (Trad et al., 2012; Ibrahim and Sacchi, 2014), deghosting (Wang et al., 2014), and microseismic data denoising (Forghani-Arani et al., 2013; Sabbione et al., 2015). Although the parabolic Radon transform can be very fast to compute in the frequency-space domain (Sacchi and Porsani, 1999), time-variant hyperbolic Radon transforms may be more appropriate to model the data. This has recently motivated a few works aiming to decrease the computation times of the transforms as well as to enhance their performance (Hu et al., 2013; Nikitin et al., 2016; Sabbione and Sacchi, 2016).

In this work, we first describe the theory and assumptions considered by the restricted domain hyperbolic Radon transform (RHRT; Sabbione and Sacchi, 2016) and stress its differences from the HRT. Next, we illustrate these differences and discuss how to implement the RHRT by means of an example attenuating multiples on a real CMP gather. Finally, we present the multiple removal results of a 2D marine seismic data set from the Mississippi Canyon region at the Gulf of Mexico.

Theory and method

In what follows we summarize the basic ideas of the restricted domain time Radon transform (RHRT), and introduce a few equations that are needed to describe the method. For a more detailed explanation, please refer to Sabbione and Sacchi (2016).

Under the assumption of low-dipping reflectors, seismic data can generally be approximated by a superposition of hyperbolic events via

$$d(t,x) = \sum_{v} m\left(\tau = \sqrt{t^2 - \frac{x^2}{v^2}},\, v\right), \qquad (1)$$

where t represents the traveltime, x is the source-receiver distance, τ indicates intercept traveltime, v is the velocity that characterize the curvature of the hyperbola, and $m(\tau, v)$ are the corresponding coefficients in the transformed domain. This equation defines an hyperbolic Radon transform between the data $d(t,x)$ and the velocity panel (τ, v). Equation (1) is generally referred as the forward hyperbolic Radon operator. Equivalently, we can define the adjoint hyperbolic Radon operator, which maps the seismic data into the (τ, v) domain by stacking over all possible hyperbolas:

$$m_{adj}(\tau,v) = \sum_{x} d\left(t = \sqrt{\tau^2 + \frac{x^2}{v^2}},\, x\right)\, dx\,. \qquad (2)$$

Note that the pair of equations (1) and (2) are computed by summations over the discretized t, x, τ, and v variables.

The data, the forward operator, and the Radon model in (1) can be written in matrix-vector form:

$$\boldsymbol{d} = \boldsymbol{L}\boldsymbol{m} + \boldsymbol{e}\,, \qquad (3)$$

where $\boldsymbol{L}$ represents the forward Radon operator. We have added a term $\boldsymbol{e}$ to denote the observational noise. Thus,

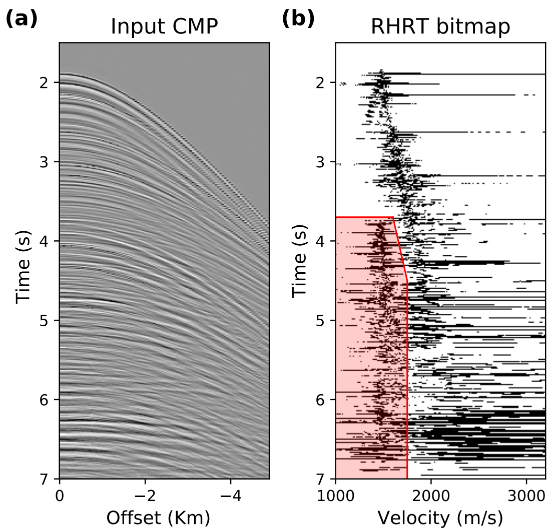

***Figure 1** – (a) CMP gather contaminated with multiples. (b) Bitmap defined by RHRT to restrict the model. The shaded red region depicts the subset used to model the multiples.*

the estimation of $m(\tau, v)$ from $d(t, x)$ can be posed as a discrete linear inverse problem (Thorson, 1985) by defining the following cost function:

$$J(\boldsymbol{m}) = \|\boldsymbol{Lm} - \boldsymbol{d}\|_2^2 + \mu \|\boldsymbol{Wm}\|_2^2 \,, \qquad (4)$$

where the weighted regularization term $\|\boldsymbol{Wm}\|$ constrains the solution. Here, μ is a trade-off parameter that balances the relative weight between the regularization term and the misfit term $\|\boldsymbol{Lm} - \boldsymbol{d}\|_2^2$. In our method, we use the information given by the adjoint coefficients m_{adj} to focus the solution on the Radon domain. Thus, we set $\boldsymbol{W} = |\boldsymbol{m}_{adj} + \varepsilon|^{-1}$, where ε is a small constant to avoid instability by zero-division. In this problem, the proposed cost function is minimized via the method of Conjugate Gradient (CG; Hestenes and Stiefel, 1952). Up to this point, we have described a method that can be referred as the classical inversion problem of the hyperbolic Radon transform (HRT).

In the RHRT (Sabbione and Sacchi, 2016), we restrict the Radon domain used to model the data by an adaptive thresholding strategy based on the adjoint coefficients given by equation (2). This technique drastically speeds up the computation of the time domain Radon transforms and improves their focusing power. As an example, let us consider the single CMP gather shown in Figure 1a. Note that the data are severely contaminated by multiples below 3.7 s. This gather belongs to the marine data set we will describe in the following sections. First, we compute the adjoint coefficients using equation (2). Next, we restrict the Radon domain by sorting the adjoint coefficients by their absolute values and selecting only those coefficients that exceed a user-defined threshold. Thereby, we construct a bitmap in the velocity panel that represents the restricted Radon domain used during the inversion (Figure 1b). In this case, only 20% of the complete Radon domain was selected. Additionally, for each CMP gather we define the sub-area of the velocity panel that models the multiples, which is represented by the shaded red region in Figure 1b. In summary, this technique conveniently permits us to model the data with a finely sampled hyperbolic time Radon transform without excessive computational cost.

RHRT vs. HRT

To complete the description of the method, we discuss the multiple attenuation results of the CMP gather showed in Figure 1a using both the HRT and the RHRT method. The CMP gather consist of 92 traces sampled at 4 ms up to $t = 7$ s. Here, we have cut the first 1.5 s of the data, which correspond to the water column. The nearest offset is at -20.72 and the farthest offset at -4874.67 m. We defined τ from 1.5 s to 7 s with $\Delta\tau = 4$ ms, and used a fine sampling of $\Delta v = 5$ m/s for the velocity with v from 1000 to 3200 m/s. We set a relatively small trade-off parameter $\mu = 0.1$ for both methods. A low value of the trade-off parameter is preferred to favor the data fitting over the regularization term in order to properly model all the multiple reflections.

The top panels in Figure 2a show the demultiple results using the classical HRT. The first panel shows the modeled velocity gathers, where the multiples were isolated with the polygon depicted in the figure. The multiples were computed using this subregion via equation (1) and are showed in the second panel. Then, the multiples were subtracted to estimate the primary reflections (third panel). Lastly, both the input CMP gather and the estimated primaries were NMO-corrected and showed in the fourth and fifth panels, respectively. These last two panels demonstrate the multiple attenuation. We also applied the RHRT and showed the results in Figure 2b (bottom panels). The Radon domain in RHRT was restricted according to Figure 1a, thus yielding computation times ten times faster than HRT for the inversion via CG. We stress that the reduced Radon domain is defined not only by the multiple subregion, but also by the bitmap strategy described in the previous section.

Although RHRT uses a significantly smaller number of coefficients than HRT, both methods yield very similar results. Moreover, remaining multiple energy (non-flat events) can be observed in the NMO-corrected estimated primaries with HRT within times between 5.5 and 7 s, whereas all events look flat after applying RHRT. Therefore, due to its better focusing power, RHRT seems to attenuate the multiples more properly than HRT. Figure 2 demonstrate that RHRT can successfully and efficiently remove multiples from the data without using the complete domain.

Results

We applied the RHRT to suppress multiples in a marine data set from the well-studied Mississippi Canyon region of the Gulf of Mexico. This 2D data set was released two decades ago by Western Geophysical for testing and benchmarking different multiple attenuation techniques. The multiple attenuation processing of this data set was addressed in several works, including Verschuur and Prein (1999), Sava and Guitton (2005), and Brown and Guitton (2005). The 2D data were acquired recording 810 shots with 183 receivers per shot, with the receivers arrays placed at the left of the source locations. Both shots and receivers separations are 26.67 m. Thus, the maximum fold is 92 traces per CMP gather. CMP numbers vary from 818

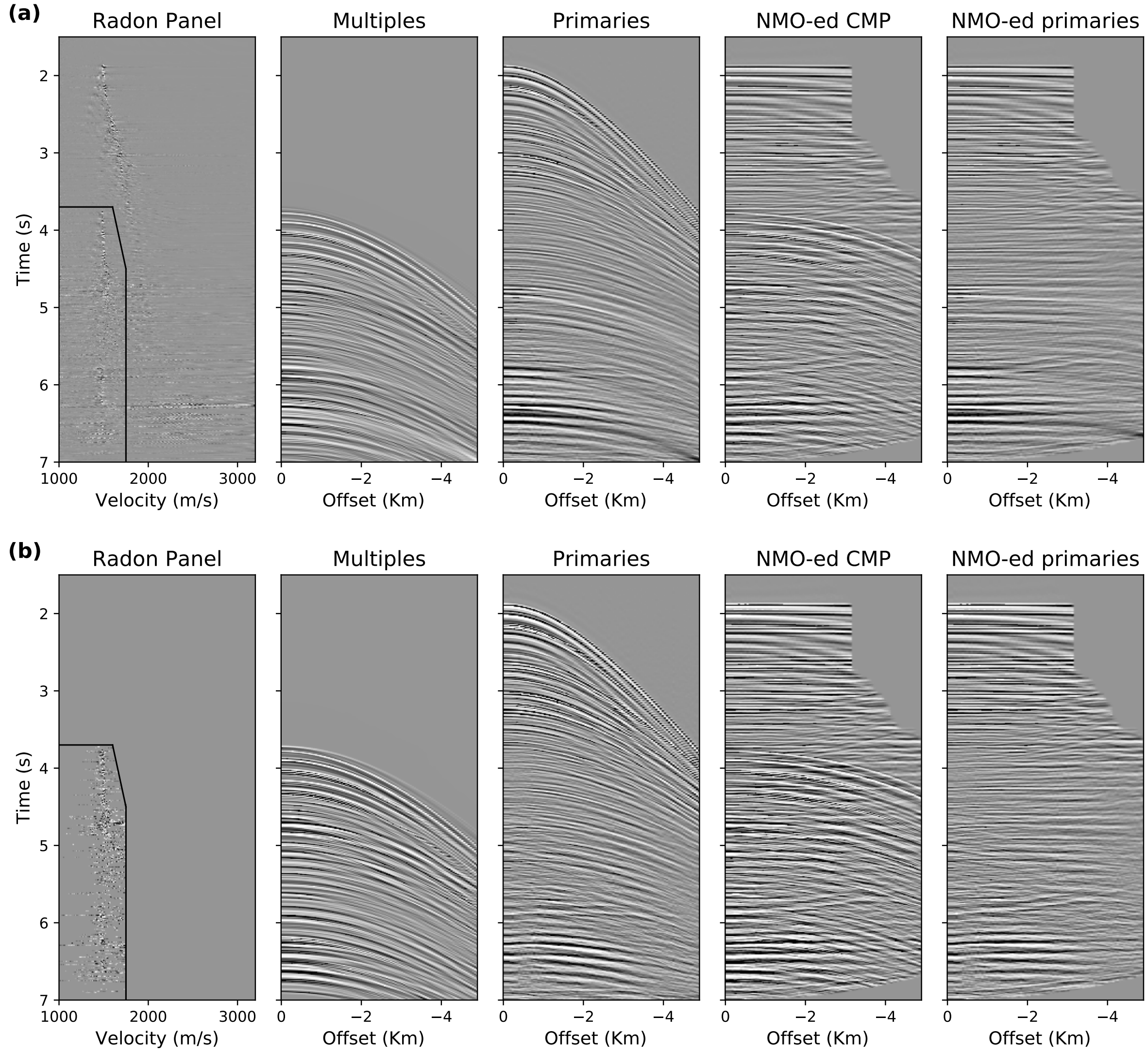

Figure 2 *– Multiple attenuation of a CMP gather using HRT and RHRT. (a) Results using HRT. (b) Results using RHRT. First panels: velocity panel and subset defined to model the multiples; second panels: estimated multiples; third panels: estimated primaries; fourth panels: input CMP after NMO correction; and fifth panels: estimated primaries after NMO correction.*

to 2618, and the first CMP with complete fold containing a nearest offset trace corresponds to CMP 1000.

This Mississippi Canyon region is well-known for the severe problems of multiples generated by the free-surface and by a shallow salt body intrusion with high reflectivity contrast. In this scenario, several multiple reflection and peglegs impinge the image of the primary reflectors. Since the multiples are partially attenuated during stacking, the optimal data to observe the multiples is given by the near-offset traces. Figure 3 shows the input near-offset section, that clearly exhibits all the multiple reflections impinging the data. Additionally, adjacent to the near-offset section, we display the NMO corrected CMP gather number 1000, which contains the first trace of the near-offset section and demonstrate the presence of the multiples in the input data. We have also annotated in the figure the main first order multiple reflections and peglegs that mask the primary reflectors and the diffractions.

We applied the RHRT to the 1801 CMP gathers that compose the entire data set of the Gulf of Mexico - Mississippi Canyon region. The same parameterization described in the CMP gather example shown in Figure 2 was used for each CMP gather. The subregions that model the multiples by polygons were set ad hoc by dividing the data into a few groups of adjacent CMP gathers. The processing carried out in this work was done in Julia using tools from the Seismic.jl package (Stanton and Sacchi, 2016), except for the NMO correction, which was computed with Seismic Unix (Cohen and Stockwell, 2007).

Figure 4 shows the same data depicted in Figure 3 after multiple removal. As a result of the processing, most of the energy produced by the multiple reflections was removed for the near offsets. The filtered near-offset section reveals great details on primary reflections and diffractions that were originally obscured by the multiples and peglegs.

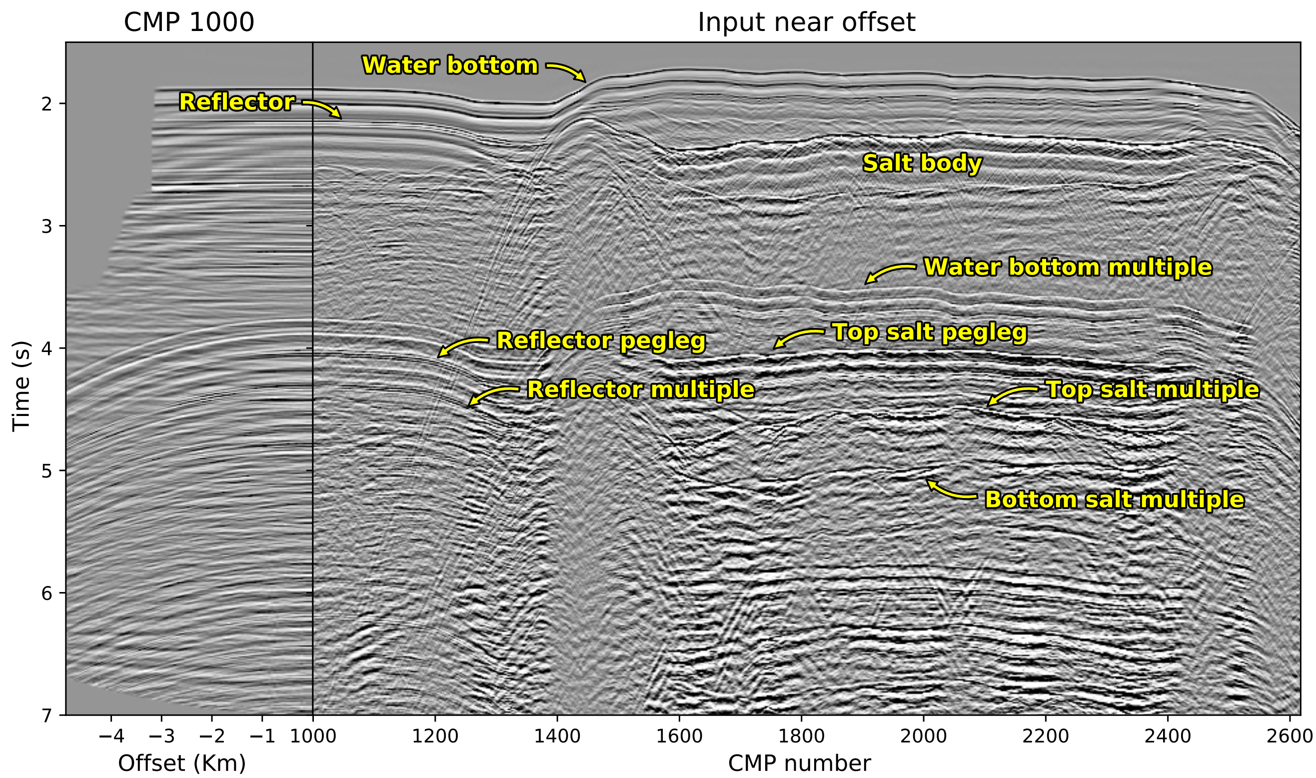

***Figure 3** – Gulf of Mexico raw near-offset section for CMP gathers* 1000 – 2618 *along with the complete CMP gather number* 1000 *that shares the first trace of the section. The main events are tagged in the plot for reference.*

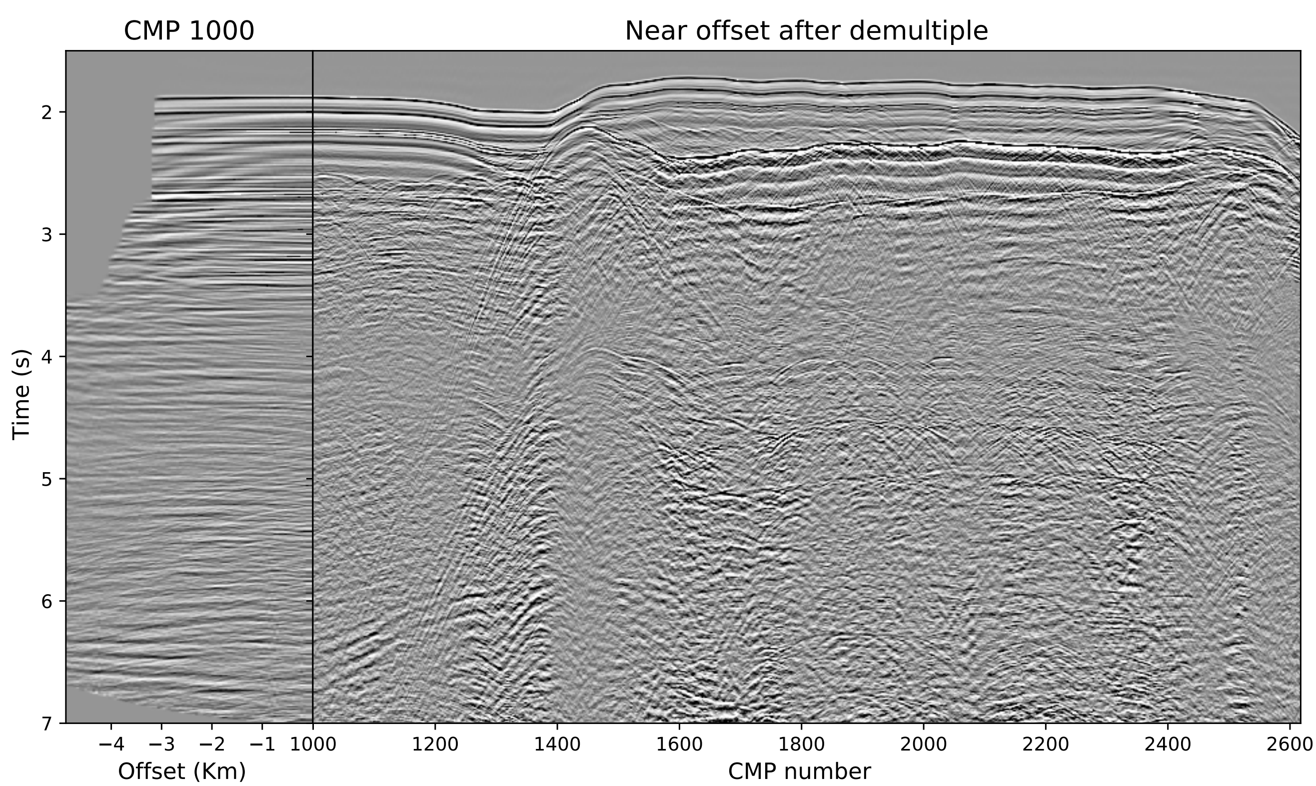

***Figure 4** – Gulf of Mexico near-offset section for CMP gathers* 1000 – 2618 *along with the complete CMP gather number* 1000 *that shares the first trace of the section after the demultiple processing. Most of the multiples were removed.*

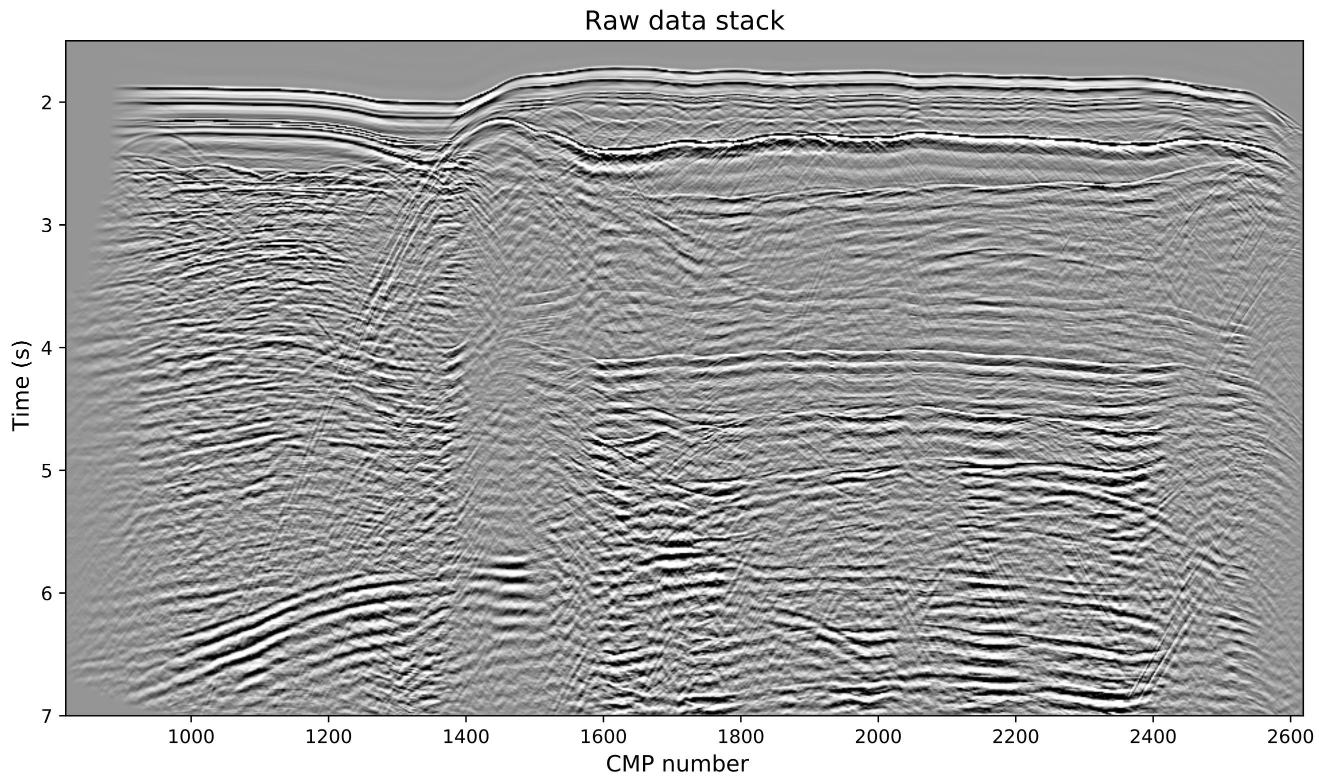

Figure 5 *– Gulf of Mexico raw stack gather before multiple attenuation. The stacking partially attenuates the multiples events but the remaining energy of the multiples and peglegs severely contaminates the data below* 3.4 *s.*

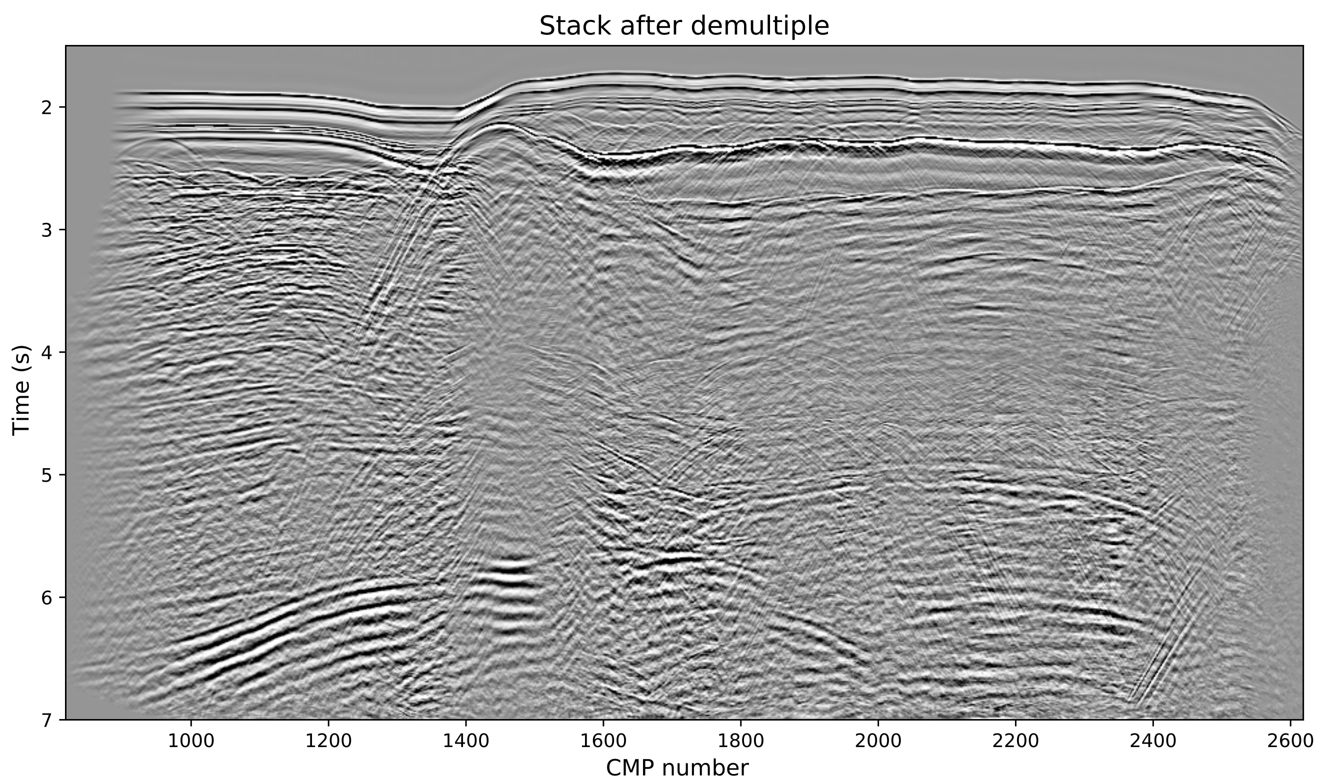

Figure 6 *– Gulf of Mexico stack gather after multiple attenuation with RHRT. Most of the multiples and peglegs observed in Figure 5 were removed. Deep primary reflections and diffractions are more continuous and noticeable.*

Figure 5 shows the stack after NMO correction of the entire data set before demultiple. The stacking partially attenuated the multiple energy. However, only the tails of the multiples in the CMP domain stack out, but the apexes of the hyperbolas survive the stacking and its energy is visible in the section. In these situations with strong multiples and peglegs energy, the stack section contains much multiple energy obscuring the data (see Figure 5).

Finally, in Figure 6 we present the final stack section after multiple attenuation by RHRT. Most of the differences observed between Figure 5 and Figure 6 are remarkable and easily spotted. Moreover, a lot of detail is gained in the section after multiple removal by RHRT. For instance, the continuity of the diffractions for CMP 1350 was enhanced in the final stack after applying RHRT. Also, the diffractions produced by the multiples at the top of the salt body at times between 4 and 4.5 s and for CMPs 1600-2400 are clearly seen in Figure 6 but indistinguishable in Figure 5. Regarding the deeper part of the section, several reflectors that were masked by high order multiples emerge better imaged and with enhanced continuity after the processing.

Conclusion

We presented an alternative technique to apply the hyperbolic Radon transform for multiple attenuation. The method adopts a fast implementation of the transform based on an adaptive restriction of the model domain for each CMP gather. The restriction is defined by velocity panels bitmaps designed with the adjoint Radon coefficients, which also serve as weights for the regularization term of the cost function. The use of a restricted model domain save computation time and focus the modeling on the signal to remove.

A well-studied Gulf of Mexico 2D data set was used to test the performance of the method. A time-variant hyperbolic Radon transform with a fine sampling in the velocity dimension was used for the processing. The results demonstrate that the multiple-reflections energy that where obscuring deep low-amplitude primaries and diffractions were efficiently removed from the data by RHRT.

Acknowledgements

The authors want to thank the sponsors of the Signal Analysis and Imaging Group (SAIG) at the University of Alberta and Western Geophysical (now part of WesternGeco) for releasing the Gulf of Mexico data set. This study was also supported by the Natural Sciences and Engineering Research Council of Canada.

References

BERKHOUT, A.J. & D.J. VERSCHUUR, 1997, Estimation of multiple scattering by iterative inversion, Part I: Theoretical considerations: Geophysics, 62, 1586–1595.

BROWN, M.P. & A. GUITTON, 2005, Least-squares joint imaging of multiples and primaries: Geophysics, 70, S79–S89.

COHEN, J.K. & J.M. STOCKWELL, 2007, CWP/SU: Seismic Unix Release No. 4.0: an open source software package for seismic research and processing: Center for Wave Phenomena, Colorado School of Mines.

FORGHANI-ARANI, F.; M. WILLIS; S.S. HAINES; M. BATZLE; J. BEHURA & M. DAVIDSON, 2013, An effective noise-suppression technique for surface microseismic data: Geophysics, 78, KS85–KS95.

FOSTER, D.J. & C.C. MOSHER, 1992, Suppression of multiple reflections using the Radon transform: Geophysics, 57, 386–395.

HAMPSON, D., 1986, Inverse velocity stacking for multiple elimination: Journal of Canadian Society of Exploration Geophysics, 22, 44–55.

HESTENES, M.R. & E. STIEFEL, 1952, Methods of conjugate gradients for solving linear systems: Journal of Research of the National Bureau of Standards, 49, 409–436.

HU, J.; S. FOMEL; L. DEMANET & L. YING, 2013, A fast butterfly algorithm for generalized Radon transforms: Geophysics, 78, U41–U51.

IBRAHIM, A. & M.D. SACCHI, 2014, Simultaneous source separation using a robust Radon transform: Geophysics, 79, V1–V11.

NIKITIN, V.V.; F. ANDERSSON; M. CARLSSON & A.A. DUCHKOV, 2016, Fast hyperbolic Radon transform represented as convolutions in log-polar coordinates: ArXiv e-prints.

SABBIONE, J.I. & M.D. SACCHI, 2016, Restricted model domain time Radon transforms: Geophysics, 81, A17–A21.

SABBIONE, J.I.; M.D. SACCHI & D.R. VELIS, 2015, Radon transform-based microseismic event detection and signal-to-noise ratio enhancement: Journal of Applied Geophysics, 113, 51–63.

SACCHI, M.D. & M. PORSANI, 1999, Fast high resolution parabolic Radon transform: 69th Annual International Meeting, SEG, Expanded Abstracts, 1477–1480.

SACCHI, M.D. & T.J. ULRYCH, 1995, High-resolution velocity gathers and offset space reconstruction: Geophysics, 60, 1169–1177.

SAVA, P. & A. GUITTON, 2005, Multiple attenuation in the image space: Geophysics, 70, V10–V20.

STANTON, A. & M.D. SACCHI, 2016, Efficient geophysical research in Julia: CSEG GeoConvention 2016, 1–3.

THORSON, J.R. & J.F. CLAERBOUT, 1985, Velocity-stack and slant-stack stochastic inversion: Geophysics, 50, 2727–2741.

TRAD, D.; R. SILIQI; G. POOLE & J. BOELLE, 2012, Fast and robust deblending using apex shifted Radon transform: 82nd Annual International Meeting, SEG, Expanded Abstracts.

VERSCHUUR, D.J.; A.J. BERKHOUT & C.P.A. WAPENAAR, 1992, Adaptive surface-related multiple elimination: Geophysics, 57, 1166–1177.

VERSCHUUR, D.J. & R.J. PREIN, 1999, Multiple removal results from Delft University: The Leading Edge, 18, 86–91.

WANG, P.; S. RAY & K. NIMSAILA, 2014, 3D joint deghosting and crossline interpolation for marine single-component streamer data: 84th Annual International Meeting, SEG, Expanded Abstracts, 3594–3598.